

CORRELATION OF ANISOTROPIC FREE SWELL BEHAVIOR WITH MINERALOGY IN CLEARWATER CLAY SHALE FROM FORT McMURRAY, ALBERTA



Ramin Ghassemi
SNC-Lavalin, Kingston, Ontario, Canada

Ron Wong
Department of Civil Engineering – University of Calgary, Calgary, Alberta, Canada
Zuhtu Ozden & Farsheed Bagheri
SNC-Lavalin, Vaughan, Ontario, Canada

ABSTRACT

Swelling in shale has long been known to cause problems for structures supported on Clearwater Formation. With zones of low-density clay rich stratum, the Clearwater clay shale possesses a very high swelling potential. An investigation was conducted in the laboratory on four facies of the Clearwater clay shale formation namely, Kcc-710, Kcc-700, Kcb-650, and Kca-625 to determine the swelling potential. Special attention has been devoted to predicting the swelling potential in correlation with mineral composition. The swelling strains in orthogonal directions were measured by conducting free swell tests. X-Ray diffraction analysis was conducted to determine the mineralogical content of samples from the individual facies. By correlating the observed strains with different mineral contents, an explicit relationship among the volumetric strain, the smectite content and the elapsed time was obtained. Moreover, an examination of experimental axial and radial strains was made to determine the anisotropic behavior of the clay shale.

RÉSUMÉ

Le gonflement dans le schiste a longtemps été connu pour causer des problèmes pour les structures supportées par la formation de Clearwater. Avec des zones de strates argileuses de faible densité, le schiste argileux de Clearwater possède un potentiel de gonflement très élevé. Une étude a été menée en laboratoire sur quatre faciès de la formation argileuse de Clearwater, à savoir Kcc-710, Kcc-700, Kcb-650 et Kca-625 pour déterminer le potentiel de gonflement. Une attention particulière a été apportée à la prédiction du potentiel de gonflement en corrélation avec la composition minérale. Les contraintes de gonflement dans les directions orthogonales ont été mesurées en effectuant des tests de gonflement libre. Une analyse par diffraction des rayons X a été effectuée pour déterminer la teneur minéralogique des échantillons provenant des différents faciès. En corrélant les souches observées avec différents teneurs en minéraux, une relation explicite entre la souche volumétrique, la teneur en smectite et le temps écoulé a été obtenue. De plus, un examen des déformations axiales et radiales expérimentales a été effectué pour déterminer le comportement anisotrope du schiste.

1 INTRODUCTION

Shales are very common in North America and particularly in Alberta, oil producing reservoirs are overlain by shale formations. Marine deposited shales have been known for their tendency to swell upon adsorption of water and subsequently lose their structural integrity. Damage to roads and structures due to excess swelling of foundations constructed on shale has been well documented in the literature (e.g. Nelson and Miller, 1992).

The Clearwater clay shale, a dark grey soil with zones of low-density clay rich stratum with siltstone interbeds, possesses a very high swelling potential due to its high liquid limit. An investigation was conducted in the laboratory to determine the swelling potential. Special attention has been devoted to predicting the swelling potential in correlation with soil indices and mineral composition.

Four facies of the Clearwater clay shale formation, from near Fort McMurray, Alberta, Canada, were investigated, namely, Kcc-710 facies (glaucinitic sandy clay), Kcc-700

facies (low-density clay to silty clay), Kcb-650 facies (glaucinitic sandy/silty clay), and Kca-625 facies (Silt dark grey clay to clayey silt). The swelling strains in orthogonal directions were measured by conducting free swell tests.

X-Ray diffraction analysis was conducted to determine the mineralogical content of samples from the individual facies, followed by correlating the observed strains with different mineral contents. An explicit relationship among the volumetric strain, the smectite content, and the elapsed time was obtained. An examination of experimental axial and radial strains was made to determine the anisotropic behavior of the clay shale. This paper presents the findings of the investigation.

2 MATERIAL

Geological cross section at Fort McMurray area in Alberta consists of Holocene (postglacial) and Pleistocene (glacial) deposits, overlying Cretaceous Clearwater Formation clay shale (Kc-facies) and McMurray Formation oil sand, which

are underlain by Devonian limestone. Discontinuous layers of indurated siltstone or sandstone are found in Clearwater Formation clay shale (Moore, 2007).

The Clearwater clay shale is usually dark grey with zones of low-density clay rich strata and siltstones. The clay fraction is composed of mainly illite, with lesser amounts of kaolinite, smectite, and chlorite. The clay shale is classified as having a very high potential for expansion and swelling, based on its high liquid limit (Mimura, 1990; Holtz, et al., 2010). Ghassemi and Wong (2016) has investigated the time-dependent characteristics of Clearwater shale facies using the stress relaxation tests.

Four facies of the Clearwater clay shale formation, from near Fort McMurray, Alberta, were investigated in the present study: Kcc-710 facies (glauconitic sandy clay and the shallowest facies), Kcc-700 (low-density clay to silty clay), Kcb-650 (glauconitic sandy/silty clay), and Kca-625 facies (silty dark grey clay to clayey silt and the deepest facies). Table 1 shows the facies that will be investigated in this study. All of these four facies had been deposited in an offshore environment.

Table 1. Facies classification (Moore, 2007)

Facies	Description	Description
Kcc 710	Glauconitic sandy clay	Silty-mud with fine-grained glauconitic sand interbeds and interlaminae. Sand decreases upward. Lower boundary is commonly marked by the presence of Glossifungites surface.
Kcb 700	Low density clay to silty clay	Dark grey to black, fissile low-density clay with rare to moderate silt laminae/lenses.
Kcb 650	Glauconitic sandy/silty clay	Consist of glauconitic light, medium greenish grey sandy-silty clay. Overlain by black, low-density clay marking the Wabiskaw/Clearwater boundary.
Kca 625	Silt to clay	Silt dark grey clay to clayey silt. Generally laminated with churned silt-rich laminae/lenses. Minor glauconite.

3 MINERALOGY

Shale generally contains quartz, feldspar, micacalcite, iron minerals, clay minerals (illite, smectite, chlorite and kaolinite) and organic matter. High percentage of illite and smectite in a shale leads to lower shear strengths and higher swelling potential than a shale with a high percentage of kaolinite and/or only low percentage of illite,

smectite, or other mixed-layer minerals (Underwood, 1967).

The behavior of shale is largely controlled by amount and type of its clay minerals. Clay content determines the specific surface area of soils and thus their plasticity is dependent to a great extent by clay content. Results of tests on illite-rich shale recovered from the Wilcox formation showed that permeability depends on clay content (Kuвано, et al., 2000; Kwon, et al., 2004). Dependence of elastic parameters on clay content had been reported elsewhere in literature (Vanorio, et al., 2003).

Different methods had been used to determine the amount and type of clay minerals of shale such as X-ray diffraction (XRD), scanning electron microscopy (SEM), dielectric constant measurement (DCM), and cation exchange capacity (CEC). XRD was used for semi-quantitative mineralogical analysis of the different facies of the Cretaceous Clearwater Formation.

3.1 X-ray diffraction (XRD) analysis

In this method, X-rays are used to probe the crystal structure of minerals. The various atoms in a mineral are ordered in a regular fashion and form layers with a definite interatomic spacing. From the difference in the paths travelled by the X-rays reflected by the various layers of the crystal, the diffraction angle is calculated (based on the Bragg's Law). The intensities of the diffracted X-rays as a function of measured angle for each mineral are unique and thus the mineralogical composition of each sample can be identified (Mah, 2005). Details of principle and application of this method can be found in literature (Reynolds, 1989a; Reynolds, 1989b; Srodoi, et al., 2001; Harris and Norman, 2008; Hubert, et al., 2009).

A total of twenty-four samples, six samples from each facies, were used for XRD analyses. Two types of XRD analyses, bulk sample analysis and clay fraction analysis, were carried out on each sample. The bulk sample analyses were conducted on powder samples. This analysis identifies the clay and non-clay minerals and the relative proportions of clay and non-clay minerals in each sample. Samples of less than 2 µm were used for the clay fraction analyses.

Detailed results of XRD analyses on twenty-four samples from facies of Clearwater clay shale could be found at Ghassemi (2016). Average values based on the results of analyses on samples from each facies are presented in the next section.

3.2 XRD analyses results

Detailed mineralogy of each sample of clay shale was obtained from XRD analyses. Average values for mineralogy of each facies of Clearwater clay shale from bulk sample analyses are presented in Table 2. The results of bulk sample analyses show the existence of at least 39 % of quartz (45 % in average). Other major non-clay minerals in the bulk are plagioclase (9 %), dolomite (5 %), K-feldspar (5 %), and pyrite (1 %). The clay content varies between 23 % and 45 % with an average of 34 %. Kcc-710 facies (shallowest facies) has the lowest clay content with

an average of 25 % and Kca-625 facies (deepest facies) has the highest percentage of clay (39 %). Clay content of Kcc-700 and Kcb-650 are close, 37 % and 35 %, respectively.

Average percentage of minerals constituting clay content of samples are presented in

Table 3, where the percentage of illite and smectite mixture in inter-layer is given as a whole. The same average values as the clay fractions for each facies are presented Table 4. The clay fractions are at least 55 % of illite/smectite inter-layer (66 % in average) and 11 % of illite (18 % in average) and some minor minerals, 10 % kaolinite and 5 % chlorite on average. The amount of both kaolinite and illite decreases with depth for each facies.

In

Table 5, the percentage of smectite in interlayer has been estimated. Therefore, the total percentage of illite has been reported in this table. Averages of clay fractions (smectite and illite separated) for each facies as percentage of clay fraction are presented in Table 6. Smectite, the most swelling mineral group, is 40 % of clay fraction and 14 % of the bulk in average while illite forms 44 % of clay fraction and 15 % of the bulk in average. The amount of smectite both in the bulk and as clay fraction increases with depth for each facies.

Table 2. Average mineralogy of facies of clay shale from XRD analyses

Facies	Depth (m)	Quartz (%)	K-feldspar (%)	Plagioclase	Dolomite (%)	Pyrite (%)	Clay content
Kcc-710	9.5	48	4	10	11	1	25
Kcb-700	10.9	44	6	11	1	1	37
Kcb-650	15.7	47	4	7	6	1	35
Kca-625	20.6	42	5	9	2	2	39

No Gypsum in any sample.

Table 3. Average content of clay minerals of clay shale facies from XRD analyses

Facies	Depth (m)	K	Ch	I	I-S mix	Clay content (%)
Kcc-710	9.5	3	2	5	15	25
Kcb-700	10.9	4	2	7	23	37
Kcb-650	15.7	3	2	6	25	35
Kca-625	20.6	3	2	6	28	39

K: kaolinite, Ch: chlorite, I: illite, and I-S mix: illite and smectite mixture in inter-layer.

Table 4. Average content of clay minerals of clay shale facies from XRD analyses

Facies	Depth (m)	K	Ch	I	I-S mix
Kcc-710	9.5	13	8	20	59
Kcb-700	10.9	11	7	18	64
Kcb-650	15.7	8	5	17	71
Kca-625	20.6	9	4	16	72

K: kaolinite, Ch: chlorite, I: illite, and I-S mix: illite and smectite mixture in inter-layer.

Table 5. Average content of clay minerals of facies of clay shale from XRD analyses (illite and smectite separated)

Facies	Depth (m)	K	Ch	S	Total I	Clay content (%)
Kcc-710	9.5	3	2	9	12	25
Kcb-700	10.9	4	2	14	16	37
Kcb-650	15.7	3	2	15	15	35
Kca-625	20.6	3	2	18	17	39

K: kaolinite, Ch: chlorite, Total I: illite in and out of interlayer mixture with smectite, and S: smectite in inter-layer

Table 6. Average content of clay minerals of facies of clay shale from XRD analyses (illite and smectite separated)

Facies	Depth (m)	K	Ch	S	Total I
Kcc-710	9.5	13	8	34	46
Kcb-700	10.9	11	7	37	44
Kcb-650	15.7	8	5	44	43
Kca-625	20.6	9	4	45	42

K: kaolinite, Ch: chlorite, Total I: illite in and out of interlayer mixture with smectite, and S: smectite in inter-layer

4 SWELL TESTS

Geomaterial swelling anisotropy can be identified by carrying out swell test. A straightforward way to do this is the free swell test. This test gives a first indication of the expandability of the candidate clay. Three samples from

each facies, with an average diameter and height of 62 and 50 mm, respectively, were prepared for free swell tests. Then, the sample and two circular perforated plastic plates, attached to each end of the sample, were enclosed in a membrane. Finally, the samples were submerged in water. The height, diameter, and mass of the samples were measured and recorded over specific time intervals. Based on recorded data, strains in axial and two perpendicular radial directions were calculated. Then, the volumetric strain was calculated from axial and radial strains.

The variation of volumetric strains with time is very close to a power function of time (Figure 1):

$$\varepsilon_V = at^b \quad [1]$$

where, ε_V is the volumetric strain. t is the time from the start of the test in days and “ a and b ” are experimental coefficients. The resulting power functions of different samples are similar to one another. Hence, an attempt was made to correlate these curves with a third parameter. The clay content was initially selected as the third parameter. Graphs of volumetric strain versus clay content at different constant times were drawn, which demonstrated good linear correlation between these two parameters. Then, this procedure was repeated using smectite content as the third parameter instead of clay content that led to an even better correlation with volumetric strains at different times. Therefore, the volumetric strains and smectite contents of different samples are found to be related through the formula below at different constant times (Figure 2):

$$\varepsilon_V = cs + d \quad [2]$$

where, s is the smectite content; c and d are experimental coefficients.

In the next stage, the coefficients of trend lines (c and d) were drawn versus time. The coefficients c and d demonstrated very good power function trends with time in the following equations, respectively (Figure 3):

$$c = 1.2814t^{0.2844}, \quad R^2 = 0.93 \quad [3]$$

$$d = -4.4134t^{0.3329}, \quad R^2 = 0.97 \quad [4]$$

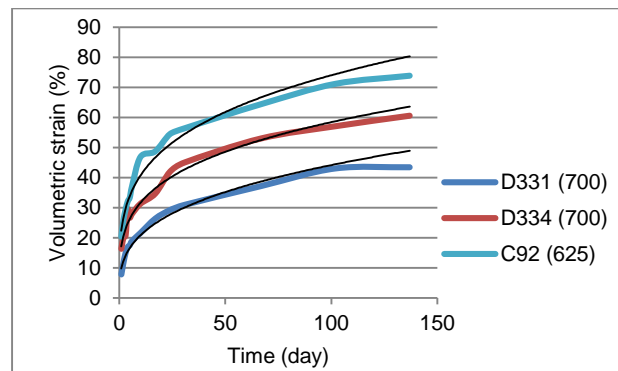


Figure 1. Variation of volumetric strains with time in free swell tests (approximated by power function)

By introducing the above equations in Eq. 2, an explicit relationship between volumetric strain with smectite content and time is obtained:

$$\varepsilon_V = (1.2814t^{0.2844})s + (-4.4134t^{0.3329}) = 1.2814st^{0.2844} - 4.4134t^{0.3329} \quad [5]$$

Volumetric strains predicted by the above formula along with measured volumetric strains are plotted versus time in Figure 4.

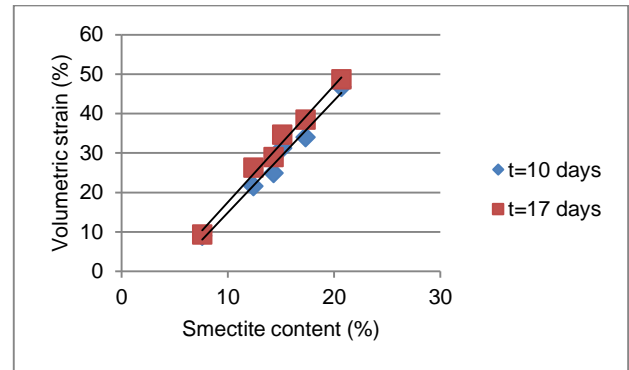


Figure 2. Linear variation of volumetric strain with smectite content in free swell tests

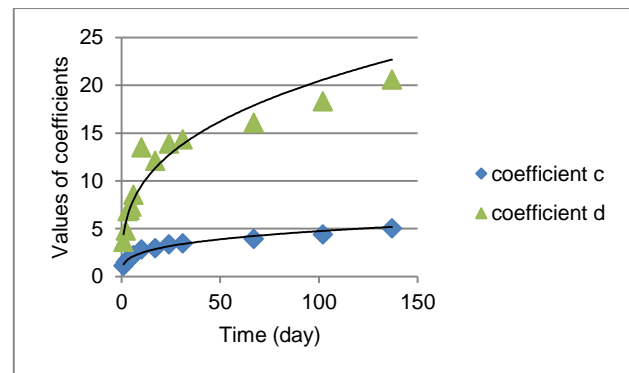


Figure 3. Power function trends of coefficients c and d with time in free swell tests

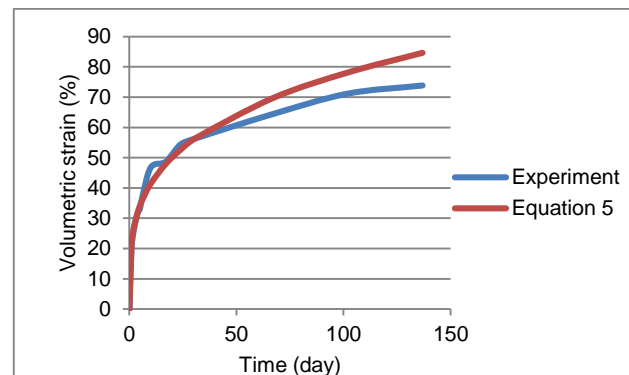


Figure 4. Comparison of experimental and predicted values of volumetric strain versus time in free swell tests (a Kca-625 facies sample)

Experimental results clearly show the anisotropic behavior of clay shale. Comparison of radial strains in two directions implies the existence of horizontal isotropy planes. Anisotropy ratio (ratio of axial strain to radial strain due to swelling) increases with smectite content (Figure 5) and decreases with time (Figure 6). The anisotropy ratios at the end of the test are between 3.45 and 4.85. There is a correlation between axial and radial strains (Figure 7):

$$\varepsilon_a = 4.715 \varepsilon_r - 4.769 \quad [6]$$

in which, ε_a is the axial strain and ε_r is the radial strain.

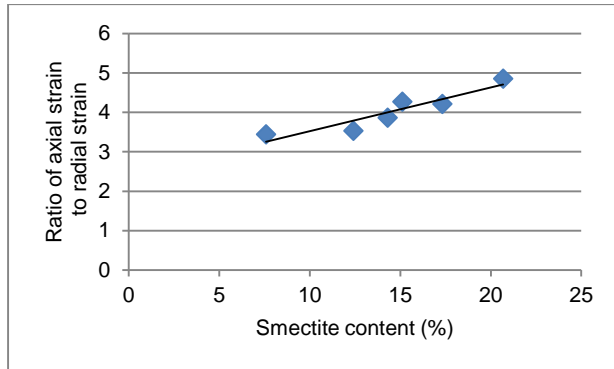


Figure 5. Variation of anisotropy ratio (ratio of axial strain to radial strain due to swelling) with smectite content in free swell tests

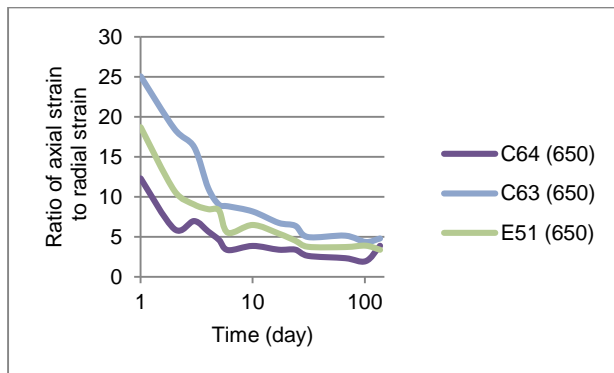


Figure 6. Variation of anisotropy ratio (ratio of axial strain to radial strain due to swelling) with time in free swell tests

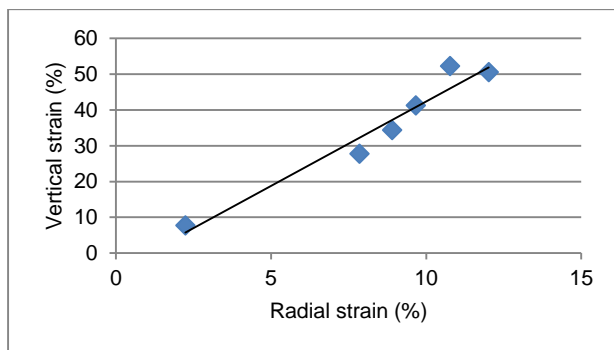


Figure 7. Correlation between axial and radial strains in free swell tests

5 DISCUSSION

5.1 Swelling anisotropy and its variation with smectite content

The performed free swell tests demonstrated the anisotropic nature of the swelling behavior of Clearwater clay shale. Moreover, the results of these tests showed the dependence of swelling potential (Figure 2) and swelling anisotropy (Figure 5) on clay content and smectite content. Hicher et al. (2000) demonstrated the dependence of the mechanical behavior of the clays on their structural characteristics. Sedimentary rocks, formed by deposits of clay and silt sediment, exhibit strong inherent anisotropy, which manifests itself in a directional dependence of deformation characteristics. The anisotropy is strongly related to the microstructure, in particular the existence of bedding planes which mark the limits of strata and can be easily identified by a visual examination (Pietruszczak et al., 2002). Considering the origin of formation of Clearwater clay shale, deposition in a shallow marine environment (Kosar, 1992), and approximately horizontal bedding planes were observed in the logging of recovered cores, anisotropy with horizontal preferential direction is expected in this material.

Avsar et al. (2009) investigated the swelling anisotropy of Ankara clay, an overconsolidated fissured clay, using a thin wall oedometer ring (providing synchronized measurement of swelling parameters in both directions). They measured greater swelling pressures in the direction normal to sheeting than in the direction parallel to sheeting in the scanning electron microscopy micrographs. They inferred that preferred orientation of clay plates and silt grains may cause the anisotropy of the swelling behavior. In addition, Chen and Huang (1987) also reported that swelling pressures in the direction perpendicular to the particle orientation is greater than that in the direction parallel to the particle orientation.

Considering the studies of Avsar et al. (2009) and Chen and Huang (1987), the swelling in Clearwater clay shale samples is expected to be markedly anisotropic (a large swelling anisotropy factor), i.e. swelling strains develop mostly in axial direction perpendicular to preferred orientation of clay particle cluster (radial direction). In addition, it is well-known that smectite has the most contribution to the swelling among various clay minerals (Olson and Mesri, 1970). Based on the role of preferential direction of clay plates, increase in smectite content of a sample is expected to result in both larger swelling strains, Figure 2, and more anisotropy in swelling, which in turn results in larger ratio of axial to radial swelling (larger swelling anisotropy factor), Figure 5.

5.2 Variation of swelling anisotropy with time (or swelling strain)

The results of free swell tests on Clearwater clay shale revealed reduction of the swelling anisotropy with the elapsed time or swelling strain (Figure 6). Katti and Katti (2003) investigated the swelling of Wyoming bentonite, a sodium montmorillonite clay. They measured swelling pressure at various levels of swelling (0, 25, 50, and 75 %

volumetric strains) and examined samples using scanning electron microscopy and Fourier transform infrared spectroscopy. They observed that 0 %-swelled samples are highly oriented as compared to 50 %-swelled samples although the dry compacted sample before saturation was prepared from randomly oriented particles. The clay platelets are most oriented at 0 % swelling. Then, clay platelets move apart due to swelling, which in turn leads to increased misorientation of the clay platelets. Therefore, misorientation of the clay platelets increases with increasing swelling strain.

Similarly, the variation of the anisotropy ratio with time in Figure 6 can be explained. With more elapsed time since the start of swelling (more swelling taking place), array of particle assemblages in Clearwater clay shale samples change from a predominantly radial direction to a more random distribution. As a result, the swelling anisotropy factor decreases with the elapsed time.

6 CONCLUSION

Using a straightforward laboratory test, namely free swell test, the anisotropic nature of the swelling behavior of Clearwater clay shale was demonstrated and quantified. The free swell test has been one of the most commonly used laboratory tests for getting an estimate of soil swelling potential. This study suggested that the results of the free swell test may be an indicator of anisotropic behavior of candid shale.

Mineral compositions of various facies of the Clearwater clay shale have been determined using XRD analyses. In next step, the results of conducted free swell tests were correlated with obtained mineralogy of each facies. Consequently, an explicit relationship between the swelling strain, the smectite content, and the elapsed time was obtained. Moreover, the comparison of the observed free swell behavior with estimated mineralogy of studied facies of shale demonstrated:

- Dependence of swelling potential on the clay content and the smectite content;
- Linear variation of swelling anisotropy with clay content and smectite content;
- Reduction of the swelling anisotropy with the elapsed time and the swelling strain.

ACKNOWLEDGEMENTS

This research was supported by an IPS scholarship, awarded by Natural Sciences and Engineering Research Council of Canada (NSERC) and Thurber Engineering Ltd., and the funding provided by the Department of Civil Engineering at University of Calgary.

REFERENCES

Avsar, E., Ulusay, R., and Sonmez, H. 2009. Assessments of swelling anisotropy of Ankara clay. *Engineering Geology*, 105(12):24–31

Chen, F.H., Huang, D., 1987. Lateral expansion pressure on basement walls. In *Proceedings of the 6th International Conference Expansive Soils*, New Delhi, vol. 1, pp. 55–59.

Ghassemi, R., 2016. Time-independent and time-dependent behavior of Clearwater clay shale underneath large storage tanks – laboratory testing and numerical modelling. Ph.D. thesis, University of Calgary, Calgary, Alberta.

Ghassemi, R., Wong, R.C.K., 2016. Investigation of the time-dependent behavior of Clearwater clay shale using triaxial stress relaxation tests. In 69th Canadian Geotechnical Conference–GeoVancouver 2016, Canadian Geotechnical Society and Vancouver Geotechnical Society, Vancouver, BC.

Harris, W. and Norman, W., 2008. X-ray diffraction techniques for soil mineral identification. In *Methods of Soil Analysis. Part 5. Mineralogical Methods*. Edited by A.L. Utery and L.R. Drees. SSSA Book Series, No. 5, Soil Science Society of America, Madison, Wisconsin, pp. 81-115.

Hicher, P.Y., Wahyudi, H. and Tessier, D., 2000. Microstructural analysis of inherent and induced anisotropy in clay. *Mechanics of Cohesive-frictional Materials*, 5(5): 341-371.

Holtz, R.D., Kovacs, W.D., and Sheahan, T.C., 2010. *An introduction to geotechnical engineering*. Prentice Hall, New Jersey.

Hubert, F., Caner, L., Meunier, A. and Lanson, B., 2009. Advances in characterization of the soil clay mineralogy using X-ray diffraction: from decomposition to profile fitting. *European Journal of Soil Science*, 60(6):1093-1105.

Katti, K., and Katti D., 2003. Effect of clay-water interactions on swelling in montmorillonite clay. In *American Society of Civil Engineers 16th engineering mechanics conference: Techniques for experimental analysis, instrumentation, and mechanics*, University of Washington, Seattle.

Kosar, K. M., 1992. Geotechnical properties of oil sands and related strata. Ph.D. thesis, University of Alberta, Edmonton, Alberta.

Kuwano, R., Connolly, T. and Jardine, R., 2000. Anisotropic stiffness measurements in a stress-path triaxial cell. *Geotechnical Testing Journal*, 23(2): 141-157.

Kwon, O., Kronenberg, A.K., Gangi, A.F., Johnson, B., and Herbert, B.E., 2004. Permeability of illite-bearing shale: 1. Anisotropy and effects of clay content and loading, *Journal of Geophysical Research*, Vol. 109, B10205, doi:10.1029/2004JB003052.

Mah, M., 2005. Determination of the elastic constants of orthorhombic and transversely isotropic materials: Experimental application to a kerogen rich rock. Ph.D. thesis, University of Alberta, Edmonton, Alberta.

Mimura, D. W., 1990. Shear strength of hydraulically placed clay shale. M.Sc. Thesis, University of Alberta, Edmonton, Alberta.

Moore, T., 2007. Performance evaluation of a simulated tank foundation on clay shale, MEng thesis, University of Calgary, Calgary, Alberta, Canada.

- Nelson, J.D., Miller, D.J., 1992. Expansive soils: problems and practice in foundation and pavement engineering. John Wiley & Sons, Inc., New York.
- Olson, R. E. and Mesri, G., 1970. Mechanisms controlling the compressibility of clays, *Journal of American Society of Civil Engineers*. 96(SM6): 1853-1878.
- Pietruszczak, S., Lydzba, D., and Shao J.F., 2002. Modelling of inherent anisotropy in sedimentary rocks. *International Journal of Solids and Structures*, 39(3): 637-648.
- Reynolds, R. J., 1989a. Principles and techniques of quantitative analysis of clay minerals by X-ray powder diffraction. In *Quantitative mineral analysis of clays*. Clay Minerals Society, Evergreen, pp. 4-37.
- Reynolds, R. J., 1989b. Principles of powder diffraction. In *Modern powder diffraction*. Mineralogical Society of America, Washington, District of Columbia, pp. 1-18.
- Srodoj, J., Drits, V.A., Mccarty, D.K., Hsieh, J.C.C., and Eberl, D.D., 2001. Quantitative X-ray diffraction analysis of clay-bearing rocks from random preparations. *Clays and Clay Minerals*, 49(6): 514-528.
- Underwood, L.B., 1967. Classification and identification of shales. *Journal of Soil Mechanics Foundations Division, American Society of Civil Engineers*, 93(6): 97-116.
- Vanorio, T., Prasad, M. and Nur, A., 2003. Elastic properties of dry clay mineral aggregates, suspensions. *Geophysical Journal International*, 155(1): 319-326.